

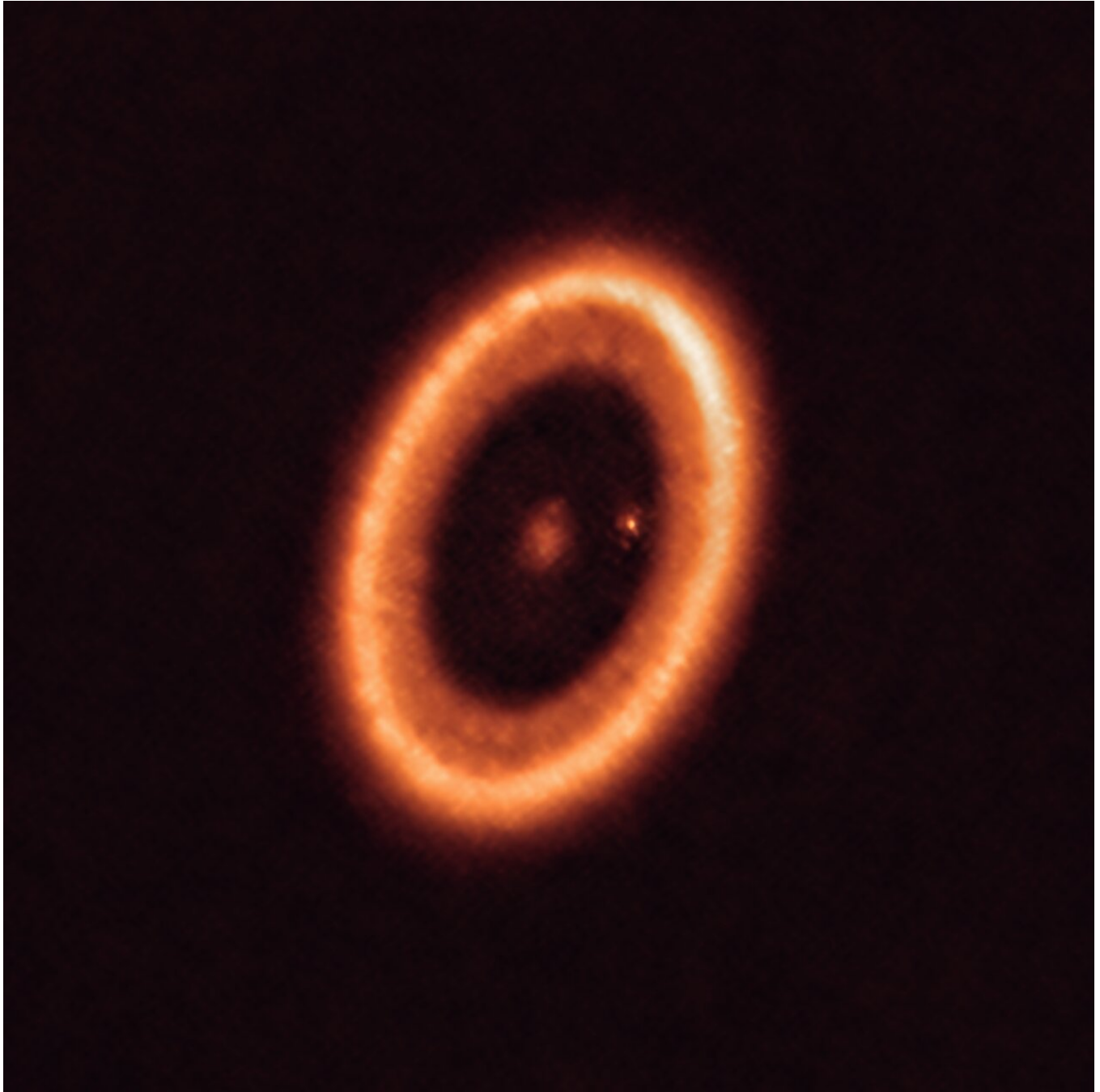
The Star Formation Newsletter

A community newsletter on Star and Planet Formation research

No. 347 — 19 November 2021

Editor: João Alves

www.starformation.news



| | | | | |
|------------|---------|-------------|------------------|---------|
| Interviews | Reviews | Perspective | Favorite objects | Archive |
| Meetings | Jobs | New PhDs | Announcements | Books |

Cover image caption

ALMA image of the PDS 70 system (resolution 20 mas, 2.3 au), located in the Sco-Cen association. The system features a star at its centre and at least two planets orbiting it, PDS 70b (not visible in the image) and PDS 70c, surrounded by a circumplanetary disc (the dot to the right of the star). The planets have carved a cavity in the circumstellar disk. Credit Benisty et al.

Note from the Editor

The Star Formation Newsletter is now on the web at www.starformation.news. This PDF file contains the monthly Abstracts and links to the different Newsletter sections. [Red text in this PDF is a url link](#). Submitting an abstract to the SFN is as simple as entering the arXiv ID (e.g., 2006.10139) in a [web form](#) on the SFN web site. **Do not remove the L^AT_EX formatting when submitting to the arXiv**. If you do, your abstract will not look great either at the arXiv or the SFN.

Abstracts

1. θ^1 Ori C as a medieval bully: a possible very recent ejection in the Trapezium

J. Maíz Apellániz, M. Pantaleoni González, R. H. Barbá ★ We use Gaia EDR3 astrometry to propose that a dynamical interaction between the multiple system θ^1 Ori C and θ^1 Ori F ejected the latter as a walkaway star 1100 years ago (without deceleration) or somewhat later (with a more likely deceleration included). It is unclear whether the final 3-D velocity of θ^1 Ori F will be large enough to escape the Orion nebula cluster.

2. Investigating variations in the dust emissivity index in the Andromeda galaxy

G. Athikkat-Eknath, S. A. Eales, M. W. L. Smith, A. Schrubba, K. A. Marsh, A. P. Whitworth ★ Over the past decade, studies of dust in the Andromeda galaxy (M31) have shown radial variations in the dust emissivity index (β). Understanding the astrophysical reasons behind these radial variations may give clues about the chemical composition of dust grains, their physical structure, and the evolution of dust. We use $^{12}\text{CO}(J=1-0)$ observations taken by the Combined Array for Research in Millimeter Astronomy (CARMA) and dust maps derived from *Herschel* images, both with an angular resolution of 8" and spatial resolution of 30 pc, to study variations in β across an area of $\approx 18.6 \text{ kpc}^2$ in M31. We extract sources, which we identify as molecular clouds, by applying the astrodendro algorithm to the ^{12}CO and dust maps, which as a byproduct allows us to compare continuum emission from dust and CO emission as alternative ways of finding molecular clouds. We then use these catalogues to investigate whether there is evidence that β is different inside and outside molecular clouds. Our results confirm the radial variations of β seen in previous studies. However, we find little difference between the average β inside molecular clouds compared to outside molecular clouds, in disagreement with models which predict an increase of β in dense environments. Finally, we find some clouds traced by dust with very little CO which may be either clouds dominated by atomic gas or clouds of molecular gas that contain little CO.

3. Supersonic Expansion of the Bipolar Hii Region Sh2-106: A 3,500 Year-Old Explosion?

John Bally, Zen Chia, Adam Ginsburg, Bo Reipurth, Kei E. I. Tanaka, Hans Zinnecker, John Faulhaber ★ Multi-epoch narrow-band HST images of the bipolar Hii region Sh2-106 reveal highly supersonic nebular proper motions which increase with projected distance from the massive young stellar object S106 IR, reaching over 30 mas/year (150 km/s at $D=1.09 \text{ kpc}$) at a projected separation of 1.4' (0.44 pc) from S106 IR. We propose that S106 IR experienced a $\sim 10^{47} \text{ erg}$ explosion 3,500 years ago. The explosion may be the result of a major accretion burst, a recent encounter with another star, or a consequence of the interaction of a companion with the bloated photosphere of S106 IR as it grew from 10 through 15 Solar masses at a high accretion rate. Near-IR images reveal fingers of molecular hydrogen emission pointing away from S106 IR.

and an asymmetric photon-dominated region surrounding the ionized nebula. Radio continuum and Brackett-gamma emission reveal a C-shaped bend in the plasma, either indicating motion of S106 IR toward the east, or deflection of plasma toward the west by the surrounding cloud. The Hii region bends around a $1'$ diameter dark bay west of S106 IR that may be shielded from direct illumination by a dense molecular clump. Herbig-Haro (HH) and Molecular Hydrogen Objects (MHOs) tracing outflows powered by stars in the Sh2-106 proto-cluster such as the Class 0 source S106 FIR are discussed.

4. Kinematics and Structure of Ionized Gas in the UCHII Regions of W33 Main

Dan Beilis, Sara Beck, John Lacy ★ High mass proto-stars create Ultra-Compact Hii regions (UCHII) at the stage of evolution when most of the accretion is finished but the star is still heavily embedded in molecular material. The morphologies of UCHII regions reflect the interactions of stellar winds, stellar motions, and density structure in the molecular cloud; they are complex and it has been very difficult to interpret them. We here present data obtained with TEXES on the NASA IRTF of the [NeII] emission line in the proto-cluster of young OB stars in W33 Main. The data cube has a spatial resolution of 1.4 arcsec and true velocity resolution 5 km/s; with $A_{\text{V}} = 0.02$ it is relatively unaffected by extinction. We have run 3D hydrodynamic and line profile simulations, using PLUTO and RADMC-3D, of the gas structures created by multiple windy stars moving relative to each other through the ambient cloud. By iterative comparison of the data cube and the simulations, we arrive at models that reproduce the different morphology and kinematic structure of each UCHII region in W33 Main. The results indicate that each sub-source probably holds multiple exciting stars, permitting an improved view of the stellar population, and finds the stellar trajectories, which may determine the dynamical development of the proto-cluster.

5. Robustness of Synthetic Observations in Producing Observed Core Properties: Predictions for the TolTEC Clouds to Cores Legacy Survey

S. K. Betti, R. Gutermuth, S. Offner, G. Wilson, A. Sokol, R. Pokhrel ★ We use hydrodynamical simulations of star-forming gas with stellar feedback and sink particles (proxies for young stellar objects, i.e., YSOs) to produce and analyze synthetic 1.1mm continuum observations at different distances (150 - 1000pc) and ages (0.49 - 1.27 Myr). We characterize how the inferred core properties, including mass, size, and clustering with respect to diffuse natal gas structure, change with distance, cloud evolution, and the presence of YSOs. We find that atmospheric filtering and core segmentation treatments have distance-dependent impacts on the resulting core properties for $d < 300$ pc and 500pc, respectively, which dominate over evolutionary differences. Concentrating on synthetic observations at further distances (650-1000pc), we find a growing separation between the inferred sizes and masses of cores with and without YSOs in the simulations, which is not seen in recent observations of the Mon R2 cloud at 860pc. We find that the synthetic cores cluster in smaller groups, and their mass densities are correlated with gas column density over a much narrower range, than the Mon R2 observations. Such differences limit applicability of the evolutionary predictions we report here and motivate future efforts to adapt our synthetic observation and analysis framework to next generation simulations such as STARFORGE. These predictions and systematic characterizations will help guide analysis of cores for the upcoming TolTEC Clouds to Cores Legacy Survey on the Large Millimeter Telescope Alfonso Serrano (LMT).

6. The Per-Tau Shell: A Giant Star-Forming Spherical Shell Revealed by 3D Dust Observations

Shmuel Bialy, Catherine Zucker, Alyssa Goodman, Michael M. Foley, João Alves, Vadim A. Semenov, Robert Benjamin, Reimar Leike, Torsten Enßlin ★ A major question in the field of star formation is how molecular clouds form out of the diffuse Interstellar Medium (ISM). Recent advances in 3D dust mapping are revolutionizing our view of the structure of the ISM. Using the highest-resolution 3D dust map to date, we explore the structure of a nearby star-forming region, which includes the well-known Perseus and Taurus molecular clouds. We reveal an extended near-spherical shell, 156 pc in diameter, hereafter the "Per-Tau Shell", in which the Perseus and Taurus clouds are embedded. We also find a large ring structure at the location of Taurus, hereafter, the "Tau Ring". We discuss a formation scenario for the Per-Tau Shell, in which previous stellar and supernova (SN) feedback events formed a large expanding shell, where the swept-up ISM has condensed to form both the shell and the Perseus and Taurus molecular clouds within it. We present auxiliary observations of HI, $H\alpha$, ^{26}Al , and X-rays that further support this scenario, and estimate Per-Tau Shell's age to be $\approx 6 - 22$ Myrs. The Per-Tau shell offers the first three-dimensional observational view of a phenomenon long-hypothesized theoretically, molecular cloud formation and star formation triggered by previous stellar and SN feedback.

7. The SEDIGISM survey: The influence of spiral arms on the molecular gas distribution of the inner Milky Way

D. Colombo, A. Duarte-Cabral, A. R. Pettitt, J. S. Urquhart, F. Wyrowski, T. Csengeri, K. R. Neralwar, F. Schuller, K. M. Menten, L. Anderson, P. Barnes, H. Beuther, L. Bronfman, D. Eden, A. Ginsburg, T. Henning, C. Koenig, M. -Y. Lee, M. Mattern, S. Medina, S. E. Ragan, A. J. Rigby, A. Sanchez-Monge, A. Traficante, A. Y. Yang, M. Wienen ★ The morphology of the Milky Way is still a matter of debate. In order to shed light on uncertainties surrounding the structure of the Galaxy, in this paper, we study the imprint of spiral arms on the distribution and properties of its molecular gas. To do so, we take full advantage of the SEDIGISM survey that observed a large area of the inner Galaxy in the $^{13}\text{CO}(2-1)$ line at an angular resolution of $28''$. We analyse the influences of the spiral arms by considering the features of the molecular gas emission as a whole across the longitude-velocity map built from the full survey. Additionally, we examine the properties of the molecular clouds in the spiral arms compared to the properties of their counterparts in the inter-arm regions. Through flux and luminosity probability distribution functions, we find that the molecular gas emission associated with the spiral arms does not differ significantly from the emission between the arms. On average, spiral arms show masses per unit length of $\sim 10^5 - 10^6 \text{ M}_{\odot} \text{ kpc}^{-1}$. This is similar to values inferred from data sets in which emission distributions were segmented into molecular clouds. By examining the cloud distribution across the Galactic plane, we infer that the molecular mass in the spiral arms is a factor of 1.5 higher than that of the inter-arm medium, similar to what is found for other spiral galaxies in the local Universe. We observe that only the distributions of cloud mass surface densities and aspect ratio in the spiral arms show significant differences compared to those of the inter-arm medium; other observed differences appear instead to be driven by a distance bias. By comparing our results with simulations and observations of nearby galaxies, we conclude that the measured quantities would classify the Milky Way as a flocculent spiral galaxy, rather than as a grand-design one.

8. Discs and outflows in the early phases of massive star formation: influence of magnetic fields and ambipolar diffusion

Benoît Commerçon, Matthias González, Raphaël Mignon-Risse, Patrick Hennebelle, Neil Vaytet ★ We study mass accretion and ejection in the vicinity of massive star forming cores using high-resolution (5 au) 3D AMR numerical simulations. We investigate the mechanisms at the origin of outflows and characterise the properties of the disc forming around massive protostars. We include both protostellar radiative feedback via PMS evolutionary tracks and magnetic ambipolar diffusion. We studied 3 different cases: purely hydrodynamical, ideal MHD, and ambipolar diffusion. In the resistive models, we investigate the effects the initial amplitude of both magnetic field and rotation have on the properties of the massive protostellar system. We use simple criteria to identify the outflow and disc material and follow their evolution as the central star accretes mass up to 20 solar mass. The outflow is completely different when magnetic fields are introduced, so that magnetic processes are the main driver of the outflow up to stellar masses of 20 solar mass. The disc properties depend on the physics included. The disc formed in the ideal and resistive runs show opposite properties in terms of plasma beta and of magnetic fields topology. While the disc in the ideal case is dominated by the magnetic pressure and the toroidal magnetic fields, the one formed in the resistive runs is dominated by the thermal pressure and has essentially vertical magnetic fields in the inner regions ($R < 200$ au). We find that magnetic processes dominate the early evolution of massive protostellar systems (< 20 solar mass) and shapes the accretion/ejection as well as the disc formation. Ambipolar diffusion is mainly at work at disc scales and regulates its properties. Our finding for the outflow and disc properties are reminiscent of low-mass star formation, suggesting that accretion and ejection in young massive and low-mass protostars are regulated by the same physical processes at the early stages.

9. Gas dynamics in the star forming region G18.148–0.283: Is it a manifestation of two colliding molecular clouds?

Jyotirmoy Dey, Jagadheep D. Pandian, Dharam Vir Lal ★ We report the results obtained from a multi-wavelength study of the HII region, G18.148–0.283, using the upgraded Giant Metre-wave Radio Telescope (uGMRT) at 1350 MHz along with other archival data. In addition to the radio continuum emission, we have detected the $\text{H}169\alpha$ and $\text{H}170\alpha$ radio recombination lines towards G18.148–0.283 using a correlator bandwidth of 100 MHz. The moment-1 map of the ionized gas reveals a velocity gradient of approximately 10 km s^{-1} across the radio continuum peaks. The ^{12}CO ($J=3-2$) molecular line data from the COHRS survey also shows the presence of two velocity components that are very close to the velocities detected in the ionized gas. The spectrum and position-velocity diagram from CO emission reveal molecular gas at an intermediate velocity range bridging the velocity components. We see mid-infrared absorption and far-infrared emission establishing the presence of a filamentary infrared dark cloud, the extent of which includes the targeted HII region. The magnetic field inferred from dust polarization is perpendicular to the filament within the HII region. We have also identified two O9 stars and 30 young stellar objects towards the target using data from the 2MASS, UKIDSS, and GLIMPSE surveys. Cumulatively, this suggests that the region is the site of a cloud-cloud collision that has triggered massive star formation and subsequent formation of an HII region.

10. The formation of massive stellar clusters in converging galactic flows with photoionisation

C. L. Dobbs, T. J. R. Bending, A. R. Pettitt, M. R. Bate ★ We have performed simulations of cluster formation along two regions of a spiral arm taken from a global Milky Way simulation, including photoionising feedback. One region is characterised by strongly converging flows, the other represents a more typical spiral arm region. We find that more massive clusters are able to form on shorter timescales for the region with strongly converging flows. Mergers between clusters are frequent in the case of the strongly converging flows and enable the formation of massive clusters. We compare equivalent clusters formed in simulations with and without ionisation. Photoionisation does not prevent massive cluster formation, but can be seen to limit the masses of the clusters. On average the mass is reduced by around 20%, but we see a large spread from ionisation having minimal difference to leading to a 50% reduction in mass. Photoionisation is also able to clear out the gas in the vicinity of the clusters on Myr timescales, which can produce clusters with larger radii that are surrounded by more massive stellar halos. We find that the ionising feedback has more impact in our second region which is less dense and has less strongly converging flows.

11. Phase space analysis of the young stellar component of the Radcliffe Wave

J. Donada, F. Figueras ★ The Radcliffe Wave is a galactic-scale structure recently proposed by J. Alves et al. (2019). The authors propose that various molecular complexes in the solar environment follow a specific alignment and displacement that make them worthy of a common origin and evolution. In this work, we first collected and analyzed the population of very young stars and open clusters around this structure. The criteria for cross-matching these star-forming tracers with the identified Radcliffe Wave cloud complexes have been defined and applied, all based on the quality of the available astrometric and photometric data. We performed a first characterization of the structure and kinematic properties of the young stellar population linked to this wave. Our conclusions, although very preliminary, are: 1) we have identified 13 open clusters, each of them physically linked to a Cloud Complex, which are probable members of the Radcliffe Wave; 2) The OB field stars do not present the elongated structure that departs from a straight line at the Sun position observed in the Cloud Complexes; 3) the vertical motion of 11 CC-OCs members associated with the Wave is not contradictory with the behaviour expected from a simple model of harmonic motion in the vertical direction, and 4) the orbits back on time neither suggest an origin associated to a point nor to a straight line in the XZ plane.

12. Testing the Potential for Radio Variability in Disks around T Tauri Stars with Observations and Chemical Modeling

C. C. Espaillat, E. Macias, J. Wendeborn, R. Franco-Hernandez, N. Calvet, A. Rilinger, L. I. Cleeves, P. D'Alessio ★ A multiwavelength observing campaign of the T Tauri star (TTS) GM Aur was undertaken in 2019 December that obtained Swift X-ray and NUV fluxes, HST NUV spectra, LCOGT ugr and TESS photometry, CHIRON H α spectra, ALMA 13CO and C18O line fluxes, and VLA 3 cm continuum fluxes taken contemporaneously over one month. The X-ray to optical observations were presented previously. Here we present the ALMA and VLA data and make comparisons to GM Aur's accretion and X-ray properties. We report no variability in the observed millimeter CO emission. Using disk chemistry models, we show that the magnitude of the changes seen in the FUV luminosity of GM Aur could lead to variation of up to 6% in CO line emission and changes in the X-ray luminosity could lead to larger changes of 25%. However, the FUV and X-ray luminosity increases must last at least 100 years in order to induce changes, which seems implausible in the TTS stage; also, these changes would be too small to be detectable by ALMA. We report no variability in the 3 cm emission observed by the VLA, showing that changes of less than a factor of 3 in the accretion rates of TTSSs do not lead to detectable changes in the mass-loss rate traced by the jet at centimeter wavelengths. We conclude that typically seen changes in the FUV and X-ray luminosities of TTSSs do not lead to observable changes in millimeter CO line emission or jet centimeter continuum emission.

13. The Effects of Starspots on Spectroscopic Mass Estimates of Low-mass Young Stars

C. Flores, M. S. Connelley, B. Reipurth, G. Duchêne ★ Magnetic fields and mass accretion processes create dark and bright spots on the surface of young stars. These spots manifest as surface thermal inhomogeneities, which alter the global temperature measured on the stars. To understand the effects and implications of these starspots, we conducted a large iSHELL high-resolution infrared spectroscopic survey of T Tauri stars in Taurus-Auriga and Ophiuchus star-forming regions. From the K band spectra, we measured stellar temperatures and magnetic field strengths using a magnetic radiative transfer code. We compared our infrared-derived parameters against literature optical temperatures and found a) a systematic temperature difference between optical and infrared observations, and b) a positive correlation between the magnetic field strengths and the temperature differences. The discrepant temperature measurements imply significant differences in the inferred stellar masses from stellar evolutionary models. To discern which temperature better predicts the mass of the star, we compared our model-derived masses against dynamical masses measured from ALMA and PdBI for a sub-sample of our sources. From this comparison we conclude that, in the range of stellar masses from 0.3 to 1.3 M_{\odot} , neither infrared nor optical temperatures perfectly reproduce the stellar dynamical masses. But, on average, infrared temperatures produce more precise and accurate

stellar masses than optical ones.

14. Binary Formation in the Orion Nebula Cluster: Exploring the Sub-stellar Limit

Matthew De Furio, Michael R. Meyer, Megan Reiter, John Monnier, Adam Kraus, Trent Dupuy ★ We present results constraining the multiplicity of the very low mass stars and sub-stellar objects in the Orion Nebula Cluster (ONC). Our sample covers primary masses $0.012\text{--}0.1M_{\odot}$ using archival Hubble Space Telescope data obtained with the Advanced Camera for Surveys using multiple filters. Studying the binary populations of clusters provides valuable constraints of how the birth environment affects binary formation and evolution. Prior surveys have shown that the binary populations of high-mass, high-density star clusters like the ONC may substantially differ from those in low-mass associations. Very low mass stellar and sub-stellar binaries at wide separations, $>20\text{AU}$, are statistically rare in the Galactic field and have been identified in stellar associations like Taurus-Auriga and Ophiuchus. They also may be susceptible to dynamical interactions, and their formation may be suppressed by feedback from on-going star formation. We implement a double point-spread function (PSF) fitting algorithm using empirical, position dependent PSF models to search for binary companions at projected separations $> 10\text{ AU}$ (25 mas). With this technique, we identify 7 very low mass binaries, 5 of which are new detections, resulting in a binary frequency of $12^{+6}_{-3.2}\%$ over mass ratios of 0.5 - 1.0 and projected separations of 20 - 200 AU. We find an excess of very low mass binaries in the ONC compared to the Galactic field, with a probability of 10^{-6} that the populations are statistically consistent. The sub-stellar population of the ONC may require further dynamical processing of the lowest binding energy binaries to resemble the field population.

15. ALMA chemical survey of disk-outflow sources in Taurus (ALMA-DOT) VI: Accretion shocks in the disk of DG Tau and HL Tau

A. Garufi, L. Podio, C. Codella, D. Segura-Cox, M. Vander Donckt, S. Mercimek, F. Bacciotti, D. Fedele, M. Kasper, J. E. Pineda, E. Humphreys, L. Testi ★ Planet-forming disks are not isolated systems. Their interaction with the surrounding medium affects their mass budget and chemical content. In the context of the ALMA-DOT program, we obtained high-resolution maps of assorted lines from six disks that are still partly embedded in their natal envelope. In this work, we examine the SO and SO₂ emission that is detected from four sources: DG Tau, HL Tau, IRAS 04302+2247, and T Tau. The comparison with CO, HCO⁺, and CS maps reveals that the SO and SO₂ emission originates at the intersection between extended streamers and the planet-forming disk. Two targets, DG Tau and HL Tau, offers clear cases of inflowing material inducing an accretion shock on the disk material. The measured rotational temperatures and radial velocities are consistent with this view. In contrast to younger Class 0 sources, these shocks are confined to the specific disk region impacted by the streamer. In HL Tau, the known accreting streamer induces a shock in the disk outskirts, and the released SO and SO₂ molecules spiral toward the star in a few hundreds years. These results suggest that shocks induced by late accreting material may be common in the disks of young star-forming regions with possible consequences on the chemical composition and mass content of the disk. They also highlight the importance of SO and SO₂ line observations to probe accretion shocks from a larger sample.

16. A SPHERE survey of self-shadowed planet-forming disks

A. Garufi, C. Dominik, C. Ginski, M. Benisty, R. G. van Holstein, Th. Henning, N. Pawellek, C. Pinte, H. Avenhaus, S. Facchini, R. Galicher, R. Gratton, F. Menard, G. Muro-Arena, J. Milli, T. Stolker, A. Vigan, M. Villenave, T. Moulin, A. Origine, F. Rigal, J. -F. Sauvage, L. Weber ★ To date, nearly two hundred planet-forming disks have been imaged with high resolution. Our propensity to study bright and extended objects is however biasing our view of the disk demography. In this work, we contribute to alleviate this bias by analyzing fifteen disks targeted with VLT/SPHERE that look faint in scattered light. Sources were selected based on a low far-IR excess from the spectral energy distribution. The comparison with the ALMA images available for a few sources shows that the scattered light surveyed by these datasets is only detected from a small portion of the disk extent. The mild anti-correlation between the disk brightness and the near-IR excess demonstrates that these disks are self-shadowed: the inner disk rim intercepts much starlight and leaves the outer disk in penumbra. Based on the uniform distribution of the disk brightness in scattered light across all spectral types, self-shadowing would act similarly for inner rims at a different distance from the star. We discuss how the illumination pattern of the outer disk may evolve with time. Some objects in the sample are proposed to be at an intermediate stage toward bright disks from the literature with either no shadow or with sign of azimuthally confined shadows.

17. Bottling the Champagne: Dynamics and Radiation Trapping of Wind-Driven Bubbles around Massive Stars

Sam Geen, Alex de Koter ★ In this paper we make predictions for the behaviour of wind bubbles around young massive stars using analytic theory. We do this in order to determine why there is a discrepancy between theoretical models that predict that winds should play a secondary role to photoionisation in the dynamics of HII regions, and observations of young HII regions that seem to suggest a driving role for winds. In particular, regions such as M42 in Orion have neutral hydrogen shells, suggesting that the ionising radiation is trapped closer to the star. We first derive formulae for wind bubble evolution in non-uniform density fields, focusing on singular isothermal sphere density fields with a power law index of -2. We find that a classical "Weaver"-like expansion velocity becomes constant in such a density distribution. We then calculate the structure of the photoionised shell around such wind bubbles, and determine at what point the mass in the shell cannot absorb all of the ionising photons emitted by the star, causing an "overflow" of ionising radiation. We also estimate perturbations from cooling, gravity, magnetic fields and instabilities, all of which we argue are secondary effects for the conditions studied here. Our wind-driven model provides a consistent explanation for the behaviour of M42 to within the errors given by observational studies. We find that in relatively denser molecular cloud environments around single young stellar sources, champagne flows are unlikely until the wind shell breaks up due to turbulence or clumping in the cloud.

18. A wind-blown bubble in the Central Molecular Zone cloud G0.253+0.016

J. D. Henshaw, M. R. Krumholz, N. O. Butterfield, J. Mackey, A. Ginsburg, T. J. Haworth, F. Nogueras-Lara, A. T. Barnes, S. N. Longmore, J. Bally, J. M. D. Kruijssen, E. A. C. Mills, H. Beuther, D. L. Walker, C. Battersby, A. Bulatek, T. Henning, J. Ott, J. D. Soler ★ G0.253+0.016, commonly referred to as "the Brick" and located within the Central Molecular Zone, is one of the densest ($\approx 10^{3-4} \text{ cm}^{-3}$) molecular clouds in the Galaxy to lack signatures of widespread star formation. We set out to constrain the origins of an arc-shaped molecular line emission feature located within the cloud. We determine that the arc, centred on $\{l_0, b_0\} = \{0.248^\circ, 0.18^\circ\}$, has a radius of 1.3 pc and kinematics indicative of the presence of a shell expanding at $5.2^{+2.7}_{-1.9} \text{ km s}^{-1}$. Extended radio continuum emission fills the arc cavity and recombination line emission peaks at a similar velocity to the arc, implying that the molecular and ionised gas are physically related. The inferred Lyman continuum photon rate is $N_{\text{LyC}} = 10^{46.0} - 10^{47.9} \text{ photons s}^{-1}$, consistent with a star of spectral type B1-O8.5, corresponding to a mass of $\approx 12 - 20 M_\odot$. We explore two scenarios for the origin of the arc: i) a partial shell swept up by the wind of an interloper high-mass star; ii) a partial shell swept up by stellar feedback resulting from in-situ star formation. We favour the latter scenario, finding reasonable (factor of a few) agreement between its morphology, dynamics, and energetics and those predicted for an expanding bubble driven by the wind from a high-mass star. The immediate implication is that G0.253+0.016 may not be as quiescent as is commonly accepted. We speculate that the cloud may have produced a $\lesssim 10^3 M_\odot$ star cluster $\gtrsim 0.4 \text{ Myr}$ ago, and demonstrate that the high-extinction and stellar crowding observed towards G0.253+0.016 may help to obscure such a star cluster from detection.

19. Molecules with ALMA at Planet-forming Scales (MAPS). IX. Distribution and Properties of the Large Organic Molecules HC_3N , CH_3CN , and $c\text{-C}_3\text{H}_2$

John D. Ilee, Catherine Walsh, Alice S. Booth, Yuri Aikawa, Sean M. Andrews, Jaehan Bae, Edwin A. Bergin, Jennifer B. Bergner, Arthur D. Bosman, Gianni Cataldi, L. Ilseore Cleaves, Ian Czekala, Viviana V. Guzmán, Jane Huang, Charles J. Law, Romane Le Gal, Ryan A. Loomis, François Ménard, Hideko Nomura, Karin I Öberg, Chunhua Qi, Kamber R. Schwarz, Richard Teague, Takashi Tsukagoshi, David J. Wilner, Yoshihide Yamato, Ke Zhang ★ The precursors to larger, biologically-relevant molecules are detected throughout interstellar space, but determining the presence and properties of these molecules during planet formation requires observations of protoplanetary disks at high angular resolution and sensitivity. Here we present 0.3" observations of HC_3N , CH_3CN , and $c\text{-C}_3\text{H}_2$ in five protoplanetary disks observed as part of the Molecules with ALMA at Planet-forming Scales (MAPS) Large Program. We robustly detect all molecules in four of the disks (GM Aur, AS 209, HD 163296 and MWC 480) with tentative detections of $c\text{-C}_3\text{H}_2$ and CH_3CN in IM Lup. We observe a range of morphologies – central peaks, single or double rings – with no clear correlation in morphology between molecule nor disk. Emission is generally compact and on scales comparable with the millimetre dust continuum. We perform both disk-integrated and radially-resolved rotational diagram analysis to derive column densities and rotational temperatures. The latter reveals 5-10 times more column density in the inner 50-100 au of the disks when compared with the disk-integrated analysis. We demonstrate that CH_3CN originates from lower relative heights in the disks when compared with HC_3N , in some cases directly tracing the disk midplane. Finally, we find good agreement between the ratio of small to large nitriles in the outer disks and comets. Our results indicate that the protoplanetary disks studied here are host to significant reservoirs of large organic molecules, and that this planet- and comet-building material can be chemically similar to that in our own Solar System. This paper is part of the MAPS special issue of the Astrophysical Journal Supplement Series.

20. Generalised transport equation of the Autocovariance Function of the density field and mass invariant in star-forming clouds

Etienne Jaupart, Gilles Chabrier ★ In this Letter, we study the evolution of the autocovariance function (ACF) of density field fluctuations in star-forming clouds and thus of the correlation length $l_c(\rho)$ of these fluctuations, which can be identified as the average size of the most correlated structures within the cloud. Generalizing the transport equation derived by Chandrasekhar (1951) for static, homogeneous turbulence, we show that the mass contained within these structures is an invariant, i.e. that the average mass contained in the most correlated structures remains constant during the evolution of the cloud, whatever dominates the global dynamics (gravity or turbulence). We show that the growing impact of gravity on the turbulent flow yields an increase of the variance of the density fluctuations and thus a drastic decrease of the correlation length. Theoretical relations are successfully compared to numerical simulations. This picture brings a robust support to star formation paradigms where the mass concentration in turbulent star-forming clouds evolves from initially large, weakly correlated filamentary structures to smaller, denser more correlated ones, and eventually to small, tightly correlated prestellar cores. We stress that the present results rely on a pure statistical approach of density fluctuations and do not involve any specific condition for the formation of prestellar cores. Interestingly enough, we show that, under average conditions typical of Milky Way molecular clouds, this invariant average mass is about a solar mass, providing an appealing explanation for the apparent universality of the IMF under such environments.

21. K2 Discovery of a Circumsecondary Disk Transiting EPIC 220208795

L. van der Kamp, D. M. van Dam, M. A. Kenworthy, E. E. Mamajek, G. Pojmański ★ Observations of the star EPIC 220208795 (2MASS J01105556+0018507) reveal a single, deep and asymmetric eclipse, which we hypothesize is due to an eclipsing companion surrounded by a tilted and inclined opaque disk, similar to those seen around V928 Tau and EPIC 204376071. We aim to derive physical parameters of the disk and orbital parameters for the companion around the primary star. The modeling is carried out using a modified version of the python package pyPplusS, and optimization is done using emcee. The period analysis makes use of photometry from ground-based surveys, where we perform a period folding search for other possible eclipses by the disk. Parameters obtained by the best model fits are used to obtain the parameter space of the orbital parameters, while the most likely period obtained is used to constrain these parameters. The best model has an opaque disk with a radius of $1.14 \pm 0.03 R_\odot$, an impact parameter of $0.61 \pm 0.02 R_\odot$, an inclination of $77.01^\circ \pm 0.03^\circ$, a tilt of $36.81^\circ \pm 0.05^\circ$ and a transverse velocity of $77.45 \pm 0.05 \text{ km s}^{-1}$. The two most likely periods are ~ 290 days and ~ 236 days, corresponding to an eccentricity of ~ 0.7 , allowing us to make predictions for the epochs of the next eclipses. All models with tilted and inclined disks result in a minimum derived eccentricity of 0.3, which in combination with the two other known small transiting disk candidates V928 Tau and EPIC 204376071, suggest that there may be a common origin for their eccentric orbits.

22. Nobeyama 45 m Local Spur CO survey. I. Giant molecular filaments and cluster formation in the Vulpecula OB association

Mikito Kohno, Atsushi Nishimura, Shinji Fujita, Kengo Tachihara, Toshikazu Onishi, Kazuki Tokuda, Yasuo Fukui, Yusuke Miyamoto, Shota Ueda, Ryosuke Kiridoshi, Daichi Tsutsumi, Kazufumi Torii, Tetsuhiro Minamidani, Kazuya Saigo, Toshihiro Handa, Hidetoshi Sano ★ We have performed new large-scale ^{12}CO , ^{13}CO , and $\text{C}^{18}\text{O } J=1-0$ observations toward the Vulpecula OB association ($l \sim 60^\circ$) as part of the Nobeyama 45 m Local Spur CO survey project. Molecular clouds are distributed over ~ 100 pc, with local peaks at the Sh 2-86, Sh 2-87, and Sh 2-88 high-mass star-forming regions in the Vulpecula complex. The molecular gas is associated with the Local Spur, which corresponds to the nearest inter-arm region located between the Local Arm and the Sagittarius Arm. We discovered new giant molecular filaments (GMFs) in Sh 2-86, with a length of ~ 30 pc, width of ~ 5 pc, and molecular mass of $\sim 4 \times 10^4 M_\odot$. We also found that Sh 2-86 contains the three velocity components at 22, 27, and 33 km s^{-1} . These clouds and GMFs are likely to be physically associated with Sh 2-86 because they have high $^{12}\text{CO } J=2-1$ to $J=1-0$ intensity ratios and coincide with the infrared dust emission. The open cluster NGC 6823 exists at the common intersection of these clouds. We argue that the multiple cloud interaction scenario, including GMFs, can explain cluster formation in the Vulpecula OB association.

23. Misaligned disks induced by infall

M. Kuffmeier, C. P. Dullemond, S. Reissl, F. G. Goicovic ★ Arc- and tail-like structures associated with disks around Herbig stars can be a consequence of infall events occurring after the initial collapse phase of a forming star. An encounter event of gas with a star can lead to the formation of a second-generation disk after the initial protostellar collapse phase. Additionally, observations of shadows in disks can be well described by a configuration of misaligned inner and outer disk, such that the inner disk casts a shadow on the outer disk. Carrying out altogether eleven 3D hydrodynamical models with the moving mesh code AREPO, we test whether a late encounter of an existing star-disk system with a cloudlet of gas can lead to the formation of an outer disk that is misaligned with respect to the primordial inner disk. Our models demonstrate that a second-generation disk with large misalignment with respect to an existing primordial disk can easily form if the infall angle is large. The second-generation outer disk is more eccentric, though the asymmetric infall also triggers eccentricity of the inner

disk of $e \approx 0.05$ to 0.1 . Retrograde infall can lead to the formation of counter-rotating disks and enhanced accretion. As the angular momentum of the inner disk is reduced, the inner disk shrinks and a gap forms between the two disks. The resulting misaligned disk system can survive for ~ 100 kyr or longer without aligning each other even for low primordial disk masses given an infall mass of $\sim 10^{-4} M_{\odot}$. A synthetic image reveals shadows in the outer disk similar to the ones observed in multiple transition disks that are caused by the misaligned inner disk. We conclude that late inclined infall onto a star-disk system leads to the formation of a misaligned outer disk. Infall might therefore be responsible for observations of shadows in at least some transition disks.

24. Star Formation Regulation and Self-Pollution by Stellar Wind Feedback

Lachlan Lancaster, Eve C. Ostriker, Jeong-Gyu Kim, Chang-Goo Kim ★ Stellar winds contain enough energy to easily disrupt the parent cloud surrounding a nascent star cluster, and for this reason have been considered candidates for regulating star formation. However, direct observations suggest most wind power is lost, and Lancaster21a,b recently proposed that this is due to efficient mixing and cooling processes. Here, we simulate star formation with wind feedback in turbulent, self-gravitating clouds, extending our previous work. Our simulations cover clouds with initial surface density $10^2 - 10^4 M_{\odot} \text{ pc}^{-2}$, and show that star formation and residual gas dispersal is complete within 2 - 8 initial cloud free-fall times. The "Efficiently Cooled" model for stellar wind bubble evolution predicts enough energy is lost for the bubbles to become momentum-driven, we find this is satisfied in our simulations. We also find that wind energy losses from turbulent, radiative mixing layers dominate losses by "cloud leakage" over the timescales relevant for star formation. We show that the net star formation efficiency (SFE) in our simulations can be explained by theories that apply wind momentum to disperse cloud gas, allowing for highly inhomogeneous internal cloud structure. For very dense clouds, the SFE is similar to those observed in extreme star-forming environments. Finally, we find that, while self-pollution by wind material is insignificant in cloud conditions with moderate density (only $\lesssim 10^{-4}$ of the stellar mass originated in winds), our simulations with conditions more typical of a super star cluster have star particles that form with as much as 1% of their mass in wind material.

25. ATOMS: ALMA Three-millimeter Observations of Massive Star-forming regions – V. Hierarchical fragmentation and gas dynamics in IRDC G034.43+00.24

Hong-Li Liu, Anandmayee Tej, Tie Liu, Namitha Issac, Anindya Saha, Paul F. Goldsmith, Jun-Zhi Wang, Qizhou Zhang, Sheng-Li Qin, Ke Wang, Shanghuo Li, Archana Soam, Lokesh Dewangan, Chang Won Lee, Pak-Shing Li, Xun-Chuan Liu, Yong Zhang, Zhiyuan Ren, Mika Juvela, Leonardo Bronfman, Yue-Fang Wu, Ken'ichi Tatematsu, Xi Chen, Di Li, Amelia Stutz, Siju Zhang, L. Viktor Toth, Qiu-Yi Luo, Feng-Wei Xu, Jinzeng Li, Rong Liu, Jianwen Zhou, Chao Zhang, Mengyao Tang, Chao Zhang, Tapas Baug, E. Mannfors, Eswaraiah Chakali, Somnath Dutta ★ We present new 3-mm continuum and molecular lines observations from the ATOMS survey towards the massive protostellar clump, MM1, located in the filamentary infrared dark cloud (IRDC), G034.43+00.24 (G34). The lines observed are the tracers of either dense gas (e.g. $\text{HCO}^+/\text{H}_2\text{CO} + \text{J} = 1-0$) or outflows (e.g. $\text{CS J} = 2-1$). The most complete picture to date of seven cores in MM1 is revealed by dust continuum emission. These cores are found to be gravitationally bound, with virial parameter, $\alpha_{\text{vir}} < 2$. At least four outflows are identified in MM1 with a total outflowing mass of $\sim 45 M_{\odot}$, and a total energy of $\sim 1 \times 10^{47}$ erg, typical of outflows from a B0-type star. Evidence of hierarchical fragmentation, where turbulence dominates over thermal pressure, is observed at both the cloud and the clump scales. This could be linked to the scale-dependent, dynamical mass inflow/accretion on clump and core scales. We therefore suggest that the G34 cloud could be undergoing a dynamical mass inflow/accretion process linked to the multiscale fragmentation, which leads to the sequential formation of fragments of the initial cloud, clumps, and ultimately dense cores, the sites of star formation.

26. Magnetic fields in star formation: a complete compilation of all the DCF estimations

Junhao Liu, Keping Qiu, Qizhou Zhang ★ The Davis-Chandrasekhar-Fermi (DCF) method provides an indirect way to estimate the magnetic field strength from statistics of magnetic field orientations. We compile all the previous DCF estimations from polarized dust emission observations and re-calculate the magnetic field strength of the selected samples with the new DCF correction factors in Liu et al. (2021). We find the magnetic field scales with the volume density as $B \propto n^{0.57}$. However, the estimated power-law index of the observed $B - n$ relation has large uncertainties and may not be comparable to the $B - n$ relation of theoretical models. A clear trend of decreasing magnetic virial parameter (i.e., increasing mass-to-flux ratio in units of critical value) with increasing column density is found in the sample, which suggests the magnetic field dominates the gravity at lower densities but cannot compete with the gravity at higher densities. This finding also indicates that the magnetic flux is dissipated at higher column densities due to ambipolar diffusion or magnetic reconnection, and the accumulation of mass at higher densities may be by mass flows along the magnetic field lines. Both sub-Alfvénic and super-Alfvénic states are found in the sample, with the average state being approximately trans-Alfvénic.

27. Chemical survey of Class I protostars with the IRAM-30m

S. Mercimek, C. Codella, L. Podio, E. Bianchi, L. Chahine, M. Bouvier, A. Lopez-Sepulcre, R. Neri, C. Ceccarelli ★ Class I protostars are a bridge between Class 0 protostars, and Class II protoplanetary disks. Recent studies show gaps and rings in the dust distribution of disks younger than 1 Myr, suggesting that planet formation may start already at the Class I stage. To understand what chemistry planets will inherit, it is crucial to characterize the chemistry of Class I sources and to investigate how chemical complexity evolves from Class 0 protostars to protoplanetary disks. The goal is twofold: to obtain a census of the molecular complexity in a sample of four Class I protostars, and to compare it with the chemical compositions of earlier and later phases of the Sun-like star formation process. We performed IRAM-30m observations towards Class I objects (L1489-IRS, B5-IRS1, L1455-IRS1, and L1551-IRS5). The column densities of the detected species are derived assuming LTE or LVG. We detected 27 species: C-chains, N-bearing, S-bearing, Si-bearing species, deuterated molecules, and iCOMs. Different spectral profiles are observed: narrow lines towards all the sources, broader lines towards L1551-IRS5, and line wings due to outflows. Narrow c-C₃H₂ emission originates from the envelope. The iCOMs in L1551-IRS5 reveal the occurrence of hot corino chemistry, with CH₃OH and CH₃CN lines originating from a compact and warm region. Finally, OCS and H₂S seem to probe the circumbinary disks in the L1455-IRS1 and L1551-IRS5 binary systems. The deuteration in terms of elemental D/H in the molecular envelopes and hot corino are derived. In addition, B5 IRS1, L1455-IRS1 and L1551-IRS5 show a low excitation methanol line, suggesting an origin from an extended structure, plausibly UV illuminated. The abundance ratios of iCOMs with respect CH₃OH measured towards the L1551-IRS5 hot corino and the deuteration in our sample are comparable to that estimated at earlier stages, as well as to that found in comets.

28. Testing Models of Triggered Star Formation with Young Stellar Objects in Cepheus OB4

Abby Mintz, Joseph L. Hora, Elaine Winston ★ OB associations are home to newly formed massive stars, whose turbulent winds and ionizing flux create H II regions rich with star formation. Studying the distribution and abundance of young stellar objects (YSOs) in these ionized bubbles can provide essential insight into the physical processes that shape their formation, allowing us to test competing models of star formation. In this work, we examined one such OB association, Cepheus OB4 (Cep OB4) - a well-suited region for studying YSOs due to its Galactic location, proximity, and geometry. We created a photometric catalog from Spitzer/IRAC mosaics in bands 1 (3.6 μ m) and 2 (4.5 μ m). We supplemented the catalog with photometry from WISE, 2MASS, IRAC bands 3 (5.8 μ m) and 4 (8.0 μ m), MIPS 24 μ m, and MMIRS near IR data. We used color-color selections to identify 821 YSOs, which we classified using the IR slope of the YSOs' spectral energy distributions (SEDs), finding 67 Class I, 103 flat spectrum, 569 Class II, and 82 Class III YSOs. We conducted a clustering analysis of the Cep OB4 YSOs and fit their SEDs. We found many young Class I objects distributed in the surrounding shell and pillars as well as a relative age gradient of unclustered sources, with YSOs generally decreasing in age with distance from the central cluster. Both of these results indicate that the expansion of the H II region may have triggered star formation in Cep OB4.

29. Star burst in W49N presumably induced by cloud-cloud collision

Ryosuke Miyawaki, Masahiko Hayashi, Tetsuo Hasegawa ★ We present high resolution observations of CS(J=1-0), H₁₃CO+ (J=1-0), and SiO(v=0:J=1-0) lines, together with the 49GHz and 86GHz continuum emissions, toward W49N carried out with Nobeyama Millimeter Array. We identified 11 CS, 8 H₁₃CO+, and 6 SiO clumps with radii of 0.1-0.5pc. The CS and H₁₃CO+ clumps are mainly divided into two velocity components, one at 4kms-1 and the other at 12kms-1, while the SiO clumps have velocities between the two components. The SiO emission is distributed toward the UCHII ring, where the 4kms-1 component clumps of CS and H₁₃CO+ also exist. The 12kms-1 component clumps of CS are detected at the east and west of the UCHII ring with an apparent hole toward the ring. The clump masses vary from $4.4 \times 10^2 M_{\odot}$ to $4.9 \times 10^4 M_{\odot}$ with the mean values of $0.94 \times 10^4 M_{\odot}$, $0.88 \times 10^4 M_{\odot}$, and $2.2 \times 10^4 M_{\odot}$ for the CS, H₁₃CO+, and SiO clumps, respectively. The total masses derived from CS, H₁₃CO+, and SiO clumps are $1.0 \times 10^5 M_{\odot}$, $0.70 \times 10^5 M_{\odot}$, and $1.3 \times 10^5 M_{\odot}$, respectively, which agree well with the corresponding virial masses of $0.71 \times 10^5 M_{\odot}$, $1.3 \times 10^5 M_{\odot}$, and $0.88 \times 10^5 M_{\odot}$, respectively. The average molecular hydrogen densities of the clumps are $0.90 \times 10^6 \text{ cm}^{-3}$, $1.4 \times 10^6 \text{ cm}^{-3}$, and $7.6 \times 10^6 \text{ cm}^{-3}$ for the CS, H₁₃CO+ and SiO clumps, respectively. The density derived from the SiO clumps seems significantly higher than those from the others, probably because the SiO emission is produced in high density shocked regions. The free fall time scale of the clumps is estimated to be $3 \times 10^4 \text{ yr}$, which gives an accretion rate of $3 \times 10^{-3} - 1 M_{\odot} / \text{yr}$ onto a stellar core. The observed clumps are, if they are undergoing free fall, capable of producing dozens of massive stars in the next 10^5 yr . We propose a view that pre-existing two clouds collided with each other almost face-on to produce the observed clumps and triggered the burst of massive star formation in W49N.

30. A cold accretion flow onto one component of a multiple protostellar system

Nadia M. Murillo, Ewine F. van Dishoeck, Alvaro Hacar, Daniel Harsono, Jes K. Jørgensen ★ Context: Gas accretion flows transport material from the cloud core onto the protostar. In multiple protostellar systems, it is not clear if the delivery mechanism is preferential or evenly distributed among the components. Aims: Gas accretion flows within IRAS16293 is explored out to 6000 AU. Methods: ALMA Band 3 observations of low-*J* transitions of HNC, cyanopolynes (HC₃N, HC₅N),

and N_2H^+ are used to probe the cloud core structure at 100 AU resolution. Additional Band 3 archival data provide low- J HCN and SiO lines. These data are compared with the corresponding higher- J lines from the PILS Band 7 data for excitation analysis. The HNC/HCN ratio is used as a temperature tracer. Results: The low- J transitions of HC_3N , HC_5N , HNC and N_2H^+ trace extended and elongated structures from 6000 AU down to 100 AU, without accompanying dust continuum emission. Two structures are identified: one traces a flow that is likely accreting toward the most luminous component of the system IRAS16293 A. Temperatures inferred from the HCN/HNC ratio suggest that the gas in this flow is cold, between 10 and 30 K. The other structure is part of an UV-irradiated cavity wall entrained by one of the outflows. The two outflows driven by IRAS16293 A present different molecular gas distributions. Conclusions: Accretion of cold gas is seen from 6000 AU scales onto IRAS16293 A, but not onto source B, indicates that cloud core material accretion is competitive due to feedback onto a dominant component in an embedded multiple protostellar system. The preferential delivery of material could explain the higher luminosity and multiplicity of source A compared to source B. The results of this work demonstrate that several different molecular species, and multiple transitions of each species, are needed to confirm and characterize accretion flows in protostellar cloud cores.

31. From Pebbles and Planetesimals to Planets and Dust: the Protoplanetary Disk–Debris Disk Connection

Joan R. Najita, Scott J. Kenyon, Benjamin C. Bromley ★ The similar orbital distances and detection rates of debris disks and the prominent rings observed in protoplanetary disks suggest a potential connection between these structures. We explore this connection with new calculations that follow the evolution of rings of pebbles and planetesimals as they grow into planets and generate dusty debris. Depending on the initial solid mass and planetesimal formation efficiency, the calculations predict diverse outcomes for the resulting planet masses and accompanying debris signature. When compared with debris disk incidence rates as a function of luminosity and time, the model results indicate that the known population of bright cold debris disks can be explained by rings of solids with the (high) initial masses inferred for protoplanetary disk rings and modest planetesimal formation efficiencies that are consistent with current theories of planetesimal formation. These results support the possibility that large protoplanetary disk rings evolve into the known cold debris disks. The inferred strong evolutionary connection between protoplanetary disks with large rings and mature stars with cold debris disks implies that the remaining majority population of low-mass stars with compact protoplanetary disks leave behind only modest masses of residual solids at large radii and evolve primarily into mature stars without detectable debris beyond 30 au. The approach outlined here illustrates how combining observations with detailed evolutionary models of solids strongly constrains the global evolution of disk solids and underlying physical parameters such as the efficiency of planetesimal formation and the possible existence of invisible reservoirs of solids in protoplanetary disks.

32. Structure of IRAS 05168+3634 star-forming region

E. H. Nikoghosyan, N. M. Azatyan, D. H. Andreasyan, D. S. Baghdasaryan ★ This study aims to determine the main physical parameters ($\text{N}(\text{H}_2)$ hydrogen column density and T_d dust temperature) of the Interstellar medium, and their distribution in the extended star-forming region, which includes IRAS 05156+3643, 05162+3639, 05168+3634, 05177+3636, and 05184+3635 sources. We also provide a comparative analysis of the properties of the Interstellar medium and young stellar objects. Analysis of the results revealed that Interstellar medium forms relatively dense condensations around IRAS sources, which are interconnected by a filament structure. In general, in sub-regions T_d varies from 11 to 24 K, and $\text{N}(\text{H}_2)$ - from 1.0 to $4.0 \times 10^{23} \text{ cm}^{-2}$. The masses of the ISM vary from 1.7×10^4 to $2.1 \times 10^5 \text{ Msol}$. All BGPSv2 objects identified in this star-forming region are located at the $\text{N}(\text{H}_2)$ maximum. The direction of the outflows, which were found in two sub-regions, IRAS 05168+3634 and 05184+3635, correlates well with the isodensities direction. The sub-regions with the highest $\text{N}(\text{H}_2)$ and Interstellar medium mass have the largest percentage of young stellar objects with Class I evolutionary stage. The wide spread of the evolutionary ages of stars in all sub-regions (from 10^5 to 10^7 years) suggests that the process of star formation in the considered region is sequential. In those sub-regions where the mass of the initial, parent molecular cloud is larger, this process is likely to proceed more actively. On the Gaia EDR3 database, it can be assumed that all sub-regions are embedded in the single molecular cloud and belong to the same star-forming region, which is located at a distance of about 1.9 kpc.

33. Rebounding Cores to Build Star Cluster Multiple Populations

G. Parmentier, A. Pasquali ★ We present a novel approach to the riddle of star cluster multiple populations. Stars form from molecular cores. But not all cores form stars. Following their initial compression, such 'failed' cores re-expand, rather than collapsing. We propose that their formation and subsequent dispersal regulate the gas density of cluster-forming clumps and, therefore, their core and star formation rates. Clumps for which failed cores are the dominant core type experience star formation histories with peaks and troughs. In contrast, too few failed cores results in smoothly decreasing star formation rates. We identify three main parameters shaping the star formation history of a clump: the star and core formation efficiencies per free-fall time, and the time-scale on which failed cores return to the clump gas. The clump mass acts as a scaling factor. We use our model to constrain the density and mass of the Orion Nebula Cluster progenitor clump, and to caution that the

star formation histories of starburst clusters may contain close-by peaks concealed by stellar age uncertainties. Our model generates a great variety of star formation histories. Intriguingly, the chromosome maps and O-Na anti-correlations of old globular clusters also present diverse morphologies. This prompts us to discuss our model in the context of globular cluster multiple stellar populations. More massive globular clusters exhibit stronger multiple stellar population patterns, which our model can explain if the formation of the polluting stars requires a given stellar mass threshold.

34. Chemical environments of 6.7 GHz methanol maser sources

Sonu Tabitha Paulson, Jagadheep D. Pandian ★ 6.7 GHz methanol masers are the brightest of class II methanol masers that are regarded as excellent signposts in the formation of young massive stars. We present here a molecular line study of 68 6.7 GHz methanol maser hosts chosen from the MMB catalogue, that have MALT90 data available. We performed (1) pixel-by-pixel study of 9 methanol maser sources that have high signal-to-noise ratio and (2) statistical study taking into account the entire 68 sources. We estimated the molecular column densities and abundances of $\text{N}_2\text{H}^+(1-0)$, $\text{HCO}^+(1-0)$, $\text{HCN}(1-0)$ and $\text{HNC}(1-0)$ lines. The derived abundances are found to be in congruence with the typical values found towards high mass star forming regions. We derived the column density and abundance ratios between these molecular species as an attempt to unveil the evolutionary stage of methanol maser sources. We found the column density and abundance ratio of HCN to HNC to increase and that of N_2H^+ to HCO^+ to decline with source evolution, as suggested by the chemical models. The HCN/HNC , $\text{N}_2\text{H}^+/\text{HCO}^+$, HNC/HCO^+ and $\text{N}_2\text{H}^+/\text{HNC}$ ratios of the methanol maser sources are consistent with them being at a later evolutionary state than quiescent phase and possibly protostellar phase, but at an earlier stage than HII regions and PDRs.

35. Galactic Star Formation with NIKA2 (GASTON): Evidence of mass accretion onto dense clumps

GASTON collaboration A. J. Rigby et al. ★ High-mass stars ($m_* \gtrsim 8 M_\odot$) play a crucial role in the evolution of galaxies, and so it is imperative that we understand how they are formed. We have used the New IRAM KIDs Array 2 (NIKA2) camera on the Institut de Radio Astronomie Millimétrique (IRAM) 30-m telescope to conduct high-sensitivity continuum mapping of $\sim 2 \text{ deg}^2$ of the Galactic plane (GP) as part of the Galactic Star Formation with NIKA2 (GASTON) large program. We have identified a total of 1467 clumps within our deep 1.15 mm continuum maps and, by using overlapping continuum, molecular line, and maser parallax data, we have determined their distances and physical properties. By placing them upon an approximate evolutionary sequence based upon $8 \mu\text{m}$ *Spitzer* imaging, we find evidence that the most massive dense clumps accrete material from their surrounding environment during their early evolution, before dispersing as star formation advances, supporting clump-fed models of high-mass star formation.

36. Arecibo-Green Bank-LOFAR Carbon Radio Recombination Line observations toward cold HI Clouds

D. Anish Rosh, W. M. Peters, K. L. Emig, P. Salas, J. B. R. Oonk, M. E. Lebrón, J. M. Dickey ★ We present results from a search for radio recombination lines in three HI self-absorbing (HISA) clouds at 750 MHz and 321 MHz with the Robert C. Byrd Green Bank Telescope (GBT), and in three Galactic Plane positions at 327 MHz with the Arecibo Telescope. We detect Carbon Recombination Lines (CRRLs) in the direction of DR4 and DR21, as well as in the galactic plane position G34.94+0.0. We additionally detect Hydrogen Recombination Lines (HRRLs) in emission in five of the six sightlines, and a Helium line at 750 MHz towards DR21. Combining our new data with 150 MHz LOFAR detections of CRRL absorption towards DR4 and DR21, we estimate the electron densities of the line forming regions by modeling the line width as a function of frequency. The estimated densities are in the range $1.4 \rightarrow 6.5 \text{ cm}^{-3}$ towards DR4, for electron temperatures $200 \rightarrow 20 \text{ K}$. A dual line forming region with densities between $3.5 \rightarrow 24 \text{ cm}^{-3}$ and $0.008 \rightarrow 0.3 \text{ cm}^{-3}$ could plausibly explain the observed line width as a function of frequency on the DR21 sightline. The central velocities of the CRRLs compare well with CO emission and HISA lines in these directions. The cloud densities estimated from the CO lines are smaller (at least a factor of 5) than those of the CRRL forming regions. It is likely that the CRRL forming and HI self-absorbing gas is located in a denser, shocked region either at the boundary of or within the CO emitting cloud.

37. Which Part of Dense Cores Feeds Material to Protostars?: The Case of L1489 IRS

Jinshi Sai, Nagayoshi Ohashi, Anaëlle J. Maury, Sébastien Maret, Hsi-Wei Yen, Yusuke Aso, Mathilde Gaudel ★ We have conducted mapping observations ($\sim 2' \times 2'$) of the Class I protostar L1489 IRS using the 7-m array of the Atacama Compact Array (ACA) and the IRAM-30m telescope in the C^{18}O 2-1 emission to investigate the gas kinematics on 1000-10,000 au scales. The C^{18}O emission shows a velocity gradient across the protostar in a direction almost perpendicular to the outflow. The radial profile of the peak velocity was measured from a C^{18}O position-velocity diagram cut along the disk major axis. The measured peak velocity decreases with radius at a radii of $\sim 1400\text{-}2900 \text{ au}$, but increases slightly or is almost constant at radii of $r \gtrsim 2900 \text{ au}$. Disk-and-envelope models were compared with the observations to understand the nature of the radial profile of the peak velocity. The measured peak velocities are best explained by a model where the specific angular momentum is

constant within a radius of 2900 au but increases with radius outside 2900 au. We calculated the radial profile of the specific angular momentum from the measured peak velocities, and compared it to analytic models of core collapse. The analytic models reproduce well the observed radial profile of the specific angular momentum and suggest that material within a radius of ~ 4000 - 6000 au in the initial dense core has accreted to the central protostar. Because dense cores are typically $\sim 10,000$ - $20,000$ au in radius, and as L1489 IRS is close to the end of mass accretion phase, our result suggests that only a fraction of a dense core eventually forms a star.

38. Collisional properties of cm-sized high-porosity ice and dust aggregates and their applications to early planet formation

Rainer R. Schr ppler, Wolf A. Landeck, J rgen Blum ★ In dead zones of protoplanetary discs, it is assumed that micrometre-sized particles grow Brownian, sediment to the midplane and drift radially inward. When collisional compaction sets in, the growing aggregates collect slower and therefore dynamically smaller particles. This sedimentation and growth phase of highly porous ice and dust aggregates is simulated with laboratory experiments in which we obtained mm- to cm-sized ice aggregates with a porosity of 90% as well as cm-sized dust agglomerates with a porosity of 85%. We modelled the growth process during sedimentation in an analytical calculation to compute the agglomerate sizes when they reach the midplane of the protoplanetary disc. In the midplane, the dust particles form a thin dense layer and gain relative velocities by, e.g., the streaming instability or the onset of shear turbulence. To investigate also these collisions, we performed additional laboratory drop tower experiments with the high-porosity aggregates formed in the sedimentary-growth experiments and determined their mechanical parameters, including their sticking threshold velocity, which is important for their further collisional evolution on their way to form planetesimals. Finally, we developed a method to calculate the packing-density-dependent fundamental properties of our dust and ice agglomerates, the Young's modulus, the Poisson ratio, the shear viscosity and the bulk viscosity from compression measurements. With these parameters, it was possible to derive the coefficient of restitution which fits our measurements. In order to physically describe these outcomes, we applied a collision model. With this model, predictions about general dust-aggregate collisions are possible.

39. Gas phase Elemental abundances in Molecular cloudS (GEMS) V. Methanol in Taurus

S. Spezzano, A. Fuente, P. Caselli, A. Vasyunin, D. Navarro-Almada, M. Rodr guez-Baras, A. Punanova, C. Vastel, V. Wakelam ★ Methanol, one of the simplest complex organic molecules in the Interstellar Medium (ISM), has been shown to be present and extended in cold environments such as starless cores. We aim at studying methanol emission across several starless cores and investigate the physical conditions at which methanol starts to be efficiently formed, as well as how the physical structure of the cores and their surrounding environment affect its distribution. Methanol and $C^{18}O$ emission lines at 3 mm have been observed with the IRAM 30m telescope within the large program "Gas phase Elemental abundances in Molecular CloudS" (GEMS) towards 66 positions across 12 starless cores in the Taurus Molecular Cloud. A non-LTE radiative transfer code was used to compute the column densities in all positions. We then used state-of-the-art chemical models to reproduce our observations. We have computed $N(CH_3OH)/N(C^{18}O)$ column density ratios for all the observed offsets, and two different behaviours can be recognised: the cores where the ratio peaks at the dust peak, and the cores where the ratio peaks with a slight offset with respect to the dust peak (~ 10000 AU). We suggest that the cause of this behaviour is the irradiation on the cores due to protostars nearby which accelerate energetic particles along their outflows. The chemical models, which do not take into account irradiation variations, can reproduce fairly well the overall observed column density of methanol, but cannot reproduce the two different radial profiles observed. We confirm the substantial effect of the environment onto the distribution of methanol in starless cores. We suggest that the clumpy medium generated by protostellar outflows might cause a more efficient penetration of the interstellar radiation field in the molecular cloud and have an impact on the distribution of methanol in starless cores.

40. The "Maggie" filament: Physical properties of a giant atomic cloud

J. Syed, J. D. Soler, H. Beuther, Y. Wang, S. Suri, J. D. Henshaw, M. Riener, S. Bialy, S. Rezaei Kh., J. M. Stil, P. F. Goldsmith, M. R. Rugel, S. C. O. Glover, R. S. Klessen, J. Kerp, J. S. Urquhart, J. Ott, N. Roy, N. Schneider, R. J. Smith, S. N. Longmore, H. Linz ★ The atomic phase of the interstellar medium plays a key role in the formation process of molecular clouds. Due to the line-of-sight confusion in the Galactic plane that is associated with its ubiquity, atomic hydrogen emission has been challenging to study. Employing the high-angular resolution data from the THOR survey, we identify one of the largest, coherent, mostly atomic HI filaments in the Milky Way at the line-of-sight velocities around -54 km/s. The giant atomic filament "Maggie", with a total length of 1.2 kpc, is not detected in most other tracers, and does not show signs of active star formation. At a kinematic distance of 17 kpc, Maggie is situated below (by 500 pc) but parallel to the Galactic HI disk and is trailing the predicted location of the Outer Arm by 5-10 km/s in longitude-velocity space. The centroid velocity exhibits a smooth gradient of less than ± 3 km/s / 10 pc and a coherent structure to within ± 6 km/s. The line widths of 10 km/s along the spine of the filament are dominated by non-thermal effects. After correcting for optical depth effects, the mass of Maggie's dense spine is estimated to be $7.2 \times 10^5 M_\odot$. The mean number density of the filament is

4 cm^{-3} , which is best explained by the filament being a mix of cold and warm neutral gas. In contrast to molecular filaments, the turbulent Mach number and velocity structure function suggest that Maggie is driven by transonic to moderately supersonic velocities that are likely associated with the Galactic potential rather than being subject to the effects of self-gravity or stellar feedback. The column density PDF displays a log-normal shape around a mean of $N_{\text{HI}} = 4.8 \times 10^{20}\text{ cm}^{-2}$, thus reflecting the absence of dominating effects of gravitational contraction.

41. **Accretion Flows or Outflow Cavities? Uncovering the Gas Dynamics around Lupus 3-MMS**

Travis J. Thieme, Shih-Ping Lai, Sheng-Jun Lin, Pou-Ieng Cheong, Chin-Fei Lee, Hsi-Wei Yen, Zhi-Yun Li, Ka Ho Lam, Bo Zhao ★ Understanding how material accretes onto the rotationally supported disk from the surrounding envelope of gas and dust in the youngest protostellar systems is important for describing how disks are formed. Magnetohydrodynamic simulations of magnetized, turbulent disk formation usually show spiral-like streams of material (accretion flows) connecting the envelope to the disk. However, accretion flows in these early stages of protostellar formation still remain poorly characterized due to their low intensity and possibly some extended structures are disregarded as being part of the outflow cavity. We use ALMA archival data of a young Class 0 protostar, Lupus 3-MMS, to uncover four extended accretion flow-like structures in C^{18}O that follow the edges of the outflows. We make various types of position-velocity cuts to compare with the outflows and find the extended structures are not consistent with the outflow emission, but rather more consistent with a simple infall model. We then use a dendrogram algorithm to isolate five sub-structures in position-position-velocity space. Four out of the five sub-structures fit well ($>95\%$) with our simple infall model, with specific angular momenta between $2.7 - 6.9 \times 10^{-4}\text{ km s}^{-1}\text{ pc}$ and mass-infall rates of $0.5 - 1.1 \times 10^{-6}\text{ M}_{\odot}\text{ yr}^{-1}$. Better characterization of the physical structure in the supposed "outflow-cavities" is important to disentangle the true outflow cavities and accretion flows.

42. **The VLA/ALMA Nascent Disk and Multiplicity (VANDAM) Survey of Orion Protostars V. A Characterization of Protostellar Multiplicity**

John J. Tobin, Stella S. R. Offner, Kaitlin M. Kratter, S. Thomas Megeath, Patrick D. Sheehan, Leslie W. Looney, Ana Karla Diaz-Rodriguez, Mayra Osorio, Guillem Anglada, Sarah I. Sadavoy, Elise Furlan, Dominique Segura-Cox, Nicole Karnath, Merel L. R. van 't Hoff, Ewine F. van Dishoeck, Zhi-Yun Li, Rajeeb Sharma, Amelia M. Stutz, Lukasz Tychoniec ★ We characterize protostellar multiplicity in the Orion molecular clouds using ALMA 0.87 mm and VLA 9 mm continuum surveys toward 328 protostars. These observations are sensitive to projected spatial separations as small as $\sim 20\text{ au}$, and we consider source separations up to 10^4 au as potential companions. The overall multiplicity fraction (MF) and companion fraction (CF) for the Orion protostars are 0.30 ± 0.03 and 0.44 ± 0.03 , respectively, considering separations from 20 to 10^4 au . The MFs and CFs are corrected for potential contamination by unassociated young stars using a probabilistic scheme based on the surface density of young stars around each protostar. The companion separation distribution as a whole is double peaked and inconsistent with the separation distribution of solar-type field stars, while the separation distribution of Flat Spectrum protostars is consistent solar-type field stars. The multiplicity statistics and companion separation distributions of the Perseus star-forming region are consistent with those of Orion. Based on the observed peaks in the Class 0 separations at $\sim 100\text{ au}$ and $\sim 10^3\text{ au}$, we argue that multiples with separations $< 500\text{ au}$ are likely produced by both disk fragmentation and turbulent fragmentation with migration, and those at 10^3 au result primarily from turbulent fragmentation. We also find that MFs/CFs may rise from Class 0 to Flat Spectrum protostars between 100 and 10^3 au in regions of high YSO density. This finding may be evidence for migration of companions from $> 10^3\text{ au}$ to $< 10^3\text{ au}$, and that some companions between 10^3 and 10^4 au must be (or become) unbound.

43. **Monte-Carlo simulations of evolving rotational distributions of low-mass stars in young open clusters. Testing the influence of initial conditions**

Maria Jaqueline Vasconcelos, Jérôme Bouvier, Florian Gallet, Edson A. Luz Filho ★ The rotational evolution of a young stellar population can give informations about the rotation pattern of more evolved clusters. Combined with rotational period values of thousands of young stars and theoretical propositions about the redistribution and loss of stellar angular momentum, it allows us to trace the rotational history of stars according to their mass. We want to investigate how internal and environmental changes on single stars can change the rotational evolution of a young stellar population. We run Monte Carlo simulations of a young cluster composed by solar mass stars of 0.5, 0.8 and 1.0 M_{\odot} from 1 to 550 Myr taking into account observational and theoretical parameters. In order to compare our results with the observations we run Kolmogorov-Smirnov tests. Our standard model is able to reproduce some clusters younger than h Per and marginally M37, which is 550 Myr old. Varying the disk fraction or the initial period distribution did not improve the results. However, when we run a model with a finer mass grid the Pleiades can be also reproduced. Changing the initial mass distribution to be similar to the empirical ONC mass function also gives good results. Modeling the evolution of a young synthetic cluster from pre-main sequence to early main sequence considering physical mechanisms of extraction and exchange of angular momentum can not be achieved successfully for all clusters for which we have enough rotational data. Clusters of about the same age present different rotational behaviors

due perhaps to differences in their initial conditions.

44. **A Kpc Scale Molecular Wave in the Inner Galaxy: Feather of the Milky Way?**

V. S. Veena, P. Schilke, Á. Sánchez-Monge, M. C. Sormani, R. S. Klessen, F. Schuller, D. Colombo, T. Csengeri, M. Mattern, J. S. Urquhart ★ We report the discovery of a velocity coherent, kpc-scale molecular structure towards the Galactic center region with an angular extent of 30deg and an aspect ratio of 60:1. The kinematic distance of the CO structure ranges between 4.4 to 6.5 kpc. Analysis of the velocity data and comparison with the existing spiral arm models support that a major portion of this structure is either a sub-branch of the Norma arm or an inter-arm giant molecular filament, likely to be a kpc-scale feather (or spur) of the Milky Way, similar to those observed in nearby spiral galaxies. The filamentary cloud is at least 2.0 kpc in extent, considering the uncertainties in the kinematic distances, and it could be as long as 4 kpc. The vertical distribution of this highly elongated structure reveals a pattern similar to that of a sinusoidal wave. The exact mechanisms responsible for the origin of such a kpc-scale filament and its wavy morphology remains unclear. The distinct wave-like shape and its peculiar orientation makes this cloud, named as the Gangotri wave, one of the largest and most intriguing structures identified in the Milky Way.

45. **Mapping physical parameters in Orion KL at high spatial resolution**

Olivia H. Wilkins, P. Brandon Carroll, Geoffrey A. Blake ★ The Orion Kleinmann-Low nebula (Orion KL) is notoriously complex and exhibits a range of physical and chemical components. We conducted high angular resolution (sub-arcsecond) observations of $^{13}\text{CH}_3\text{OH } \nu = 0$ ($\sim 0.3''$ and $\sim 0.7''$) and $\text{CH}_3\text{CN } \nu_8 = 1$ ($\sim 0.2''$ and $\sim 0.9''$) line emission with the Atacama Large Millimeter/submillimeter Array (ALMA) to investigate Orion KL's structure on small spatial scales (≤ 350 au). Gas kinematics, excitation temperatures, and column densities were derived from the molecular emission via a pixel-by-pixel spectral line fitting of the image cubes, enabling us to examine the small-scale variation of these parameters. Sub-regions of the Hot Core have a higher excitation temperature in a $0.2''$ beam than a $0.9''$ beam, indicative of possible internal sources of heating. Furthermore, the velocity field includes a bipolar $\sim 7\text{--}8 \text{ km s}^{-1}$ feature with a southeast-northwest orientation against the surrounding $\sim 4\text{--}5 \text{ km s}^{-1}$ velocity field, which may be due to an outflow. We also find evidence of a possible source of internal heating toward the Northwest Clump, since the excitation temperature there is higher in a smaller beam versus a larger beam. Finally, the region southwest of the Hot Core (Hot Core-SW) presents itself as a particularly heterogeneous region bridging the Hot Core and Compact Ridge. Additional studies to identify the (hidden) sources of luminosity and heating within Orion KL are necessary to better understand the nebula and its chemistry.

46. **Streaming Instability with Multiple Dust Species: II. Turbulence and Dust-Gas Dynamics at Nonlinear Saturation**

Chao-Chin Yang, Zhaohuan Zhu ★ The streaming instability is a fundamental process that can drive dust-gas dynamics and ultimately planetesimal formation in protoplanetary discs. As a linear instability, it has been shown that its growth with a distribution of dust sizes can be classified into two distinct regimes, fast- and slow-growth, depending on the dust-size distribution and the total dust-to-gas density ratio ϵ . Using numerical simulations of an unstratified disc, we bring three cases in different regimes into nonlinear saturation. We find that the saturation states of the two fast-growth cases are similar to its single-species counterparts. The one with maximum dimensionless stopping time $\tau_{s,\text{max}} = 0.1$ and $\epsilon = 2$ drives turbulent vertical dust-gas vortices, while the other with $\tau_{s,\text{max}} = 2$ and $\epsilon = 0.2$ leads to radial traffic jams and filamentary structures of dust particles. The dust density distribution for the former is flat in low densities, while the one for the latter has a low-end cutoff. By contrast, the one slow-growth case results in a virtually quiescent state. Moreover, we find that in the fast-growth regime, significant dust segregation by size occurs, with large particles moving towards dense regions while small particles remain in the diffuse regions, and the mean radial drift of each dust species is appreciably altered from the (initial) drag-force equilibrium. The former effect may skew the spectral index derived from multi-wavelength observations and change the initial size distribution of a pebble cloud for planetesimal formation. The latter along with turbulent diffusion may influence the radial transport and mixing of solid materials in young protoplanetary discs.